

Exact Hopfions in a 3D Heisenberg Ferromagnet

Radha Balakrishnan⁽¹⁾, Rossen Dandoloff⁽²⁾ and Avadh Saxena⁽³⁾

⁽¹⁾The Institute of Mathematical Sciences, Chennai 600 113, India

Department of Condensed Matter Physics and Microelectronics, Faculty of Physics, Sofia University, 5
Blvd. J. Bourchier, 1164 Sofia, Bulgaria

⁽³⁾Theoretical Division and Center for Nonlinear Studies, Los Alamos National Laboratory, Los Alamos,
New Mexico 87545, USA

Abstract: We find exact static soliton solutions for the unit spin vector field of an inhomogeneous, anisotropic three-dimensional (3D) Heisenberg ferromagnet. Each soliton is labeled by two integers n and m . It is a (modified) skyrmion in the $z = 0$ plane with winding number n , which twists out of the plane to become a 3D soliton. Here m arises due to the periodic boundary condition in the z direction. We use Whitehead's integral expression to find that the Hopf invariant of the soliton is an integer $H = nm$, showing that it is a hopfion. Plots of the preimages of a hopfion solution show that they are either unknots or nontrivial knots, depending on n and m . Any pair of preimage curves links H times, corroborating the interpretation of H as a linking number. We also calculate the exact hopfion energy and show that its topological lower bound has a sublinear dependence on H .

arXiv:2202.07195v1 [nlin.SI] 15 Feb 2022

Introduction. Three dimensional topological solitons called hopfions are of great current interest. They have recently been observed in magnetic [1], ferroelectric [2], liquid crystal [3, 4], and other materials, as well as studied in Bose-Einstein condensates [5, 6]. As is well known, solitons [7]–[10] are spatially localized, particle-like excitations that arise as solutions of nonlinear partial differential equations satisfied by the field configurations of the physical system concerned. A soliton can be non-topological or topological. Unlike the former, the latter is endowed with a nontrivial integer topological invariant, also called its topological charge. Since this invariant cannot be changed by a continuous deformation of the field configuration, the entity is topologically stable. This property is expected to become useful in communication technology, since these particle-like stable nonlinear entities can serve as information carriers.

Various types of Heisenberg exchange Hamiltonians for interacting spins describing a number of magnetic materials are storehouses of solitons [11]. In the static case of the classical continuum version, a normalized spin configuration at any point \mathbf{r} in physical space is described by a *unit* vector field $\mathbf{S}(\mathbf{r})$. Clearly, the tip of such a spin vector lies on a 2-sphere S^2 , irrespective of the spatial dimension in which it exists. In 2D, the topological solitons are the well known magnetic skyrmions, which are classified by an integer topological invariant $Q = (1/4\pi) \iint \mathbf{S} \cdot (\partial_x \mathbf{S} \times \partial_y \mathbf{S}) dx dy$, called the winding number [7]. First studied in 1975 by Belavin and Polyakov [12] in the context of 2D isotropic ferromagnets, they have been investigated theoretically in other magnetic models by several authors. They have also been observed experimentally in many types of 2D magnetic materials. The possible role of magnetic skyrmions as bits to store information in future computer technology has been suggested [13].

In 3D, the solitons are classified by a topological invariant called the Hopf invariant H (or Hopf charge), which is given by the Whitehead integral expression [14] [see Eq. (10) below]. A soliton with an integer H value is called a hopfion. Note that H can also be interpreted as the linking number of the two closed space curves in 3D physical space that are the preimages of any two distinct points on the target space S^2 . Magnetic materials provide an ideal platform to create and study hopfions experimentally [1]. The investigation of these topological entities as possible static solitons in 3D Heisenberg models is therefore of current interest. These arise as solutions of the variational equations minimizing the energy, the latter generically being nonlinear partial differential equations that are difficult to solve analytically. Hence

existing theoretical work on magnetic hopfions typically uses numerical methods as well as simulations [15]–[21]. These have undoubtedly yielded useful insights regarding 3D spin textures as well as the knots and links associated with them.

In the case of most micromagnetic models such as [20], the use of numerical techniques is unavoidable. On the other hand, it is instructive to identify a physically realizable magnetic model in 3D in which both the exact hopfion solution as well as its corresponding Hopf invariant can be calculated *analytically*. Analytical methods play a crucial role in clarifying the basic physical and topological characteristics of hopfions. Recently, hopfions have been created and observed experimentally in a multilayer magnetic system [1]. A solvable model can also suggest the fabrication of appropriate magnetic materials and initiate more experiments to study the various topological aspects of these nonlinear excitations. The present work is motivated by these considerations.

Our main results are as follows: We find exact static soliton solutions for the unit spin configurations $\mathbf{S}(\mathbf{r})$ of a 3D, inhomogeneous, anisotropic Heisenberg ferromagnet. Each soliton is labelled by two integers n and m . It is a modified skyrmion in the $z = 0$ plane with winding number n , which twists out of the plane to become a 3D soliton. Here m arises from the periodic boundary condition imposed in the z direction. Using the Whitehead formula [14], we calculate its Hopf charge analytically to obtain an integer $H = nm$, showing that the soliton is a hopfion ($H < 0$ corresponds to an anti-hopfion). Using the hopfion solution, we plot the preimages of a few distinct points on a specific latitude of the target space S^2 , and show that they are closed space curves that lie on a corresponding 2-torus. [$\mathbf{S}(\mathbf{r})$ points in a fixed direction on a preimage curve.] These curves are either unknots or nontrivial knots, depending on n and m . Any two of them link nm times, yielding the geometric interpretation of H as a linking number. Thus, a hopfion is associated with a twisted, knotted, linked structure. The preimages of the points on any latitude of S^2 densely fill the surface of an associated torus. We then calculate the exact energy E of the magnetic hopfion. We further find that $E \geq cH^{1/2}$ where c is a material dependent constant, establishing that the topological lower bound on E has a sublinear dependence on the Hopf charge.

Exact solitons for a 3D Heisenberg model. We consider the continuum version of a magnetic system described by the classical anisotropic (XXZ) Heisenberg ferromagnetic Hamiltonian E given by

$$E = (J/a) \iiint \{(\partial_x \mathbf{S})^2 + (\partial_y \mathbf{S})^2 + \tilde{J}_3 (\partial_z \mathbf{S})^2\} dx dy dz. \quad (1)$$

Here J is the nearest-neighbor exchange interaction in the x and y directions, $\tilde{J}_3 = J_3/J$ is the dimensionless anisotropic interaction in the z -direction, and a is the lattice constant. The unit vector \mathbf{S} is given in spherical polar coordinates by

$$\mathbf{S} = (\sin \Theta \cos \Phi, \sin \Theta \sin \Phi, \cos \Theta). \quad (2)$$

Substituting this in Eq. (1) and transforming to cylindrical coordinates (ρ, ϕ, z) in physical space, we get

$$\begin{aligned} E &= (J/a) \iiint \left\{ [(\partial_\rho \Theta)^2 + \rho^{-2} (\partial_\phi \Theta)^2] + \sin^2 \Theta [(\partial_\rho \Phi)^2 + \rho^{-2} (\partial_\phi \Phi)^2] \right. \\ &\quad \left. + \tilde{J}_3 [(\partial_z \Theta)^2 + \sin^2 \Theta (\partial_z \Phi)^2] \right\} \rho d\rho d\phi dz. \end{aligned} \quad (3)$$

We consider solutions of the form $\Theta = \Theta(\rho)$, $\Phi = \alpha_0 \phi + \beta_0 z + \Phi_0$, where the constants are to be determined by the boundary conditions on Φ . Equation (3) then reduces to

$$E = (J/a) \iiint \left\{ \rho (\partial_\rho \Theta)^2 + \alpha_0^2 \rho^{-1} \sin^2 \Theta + \tilde{J}_3 \beta_0^2 \rho \sin^2 \Theta \right\} d\rho d\phi dz. \quad (4)$$

We will show that an inhomogeneous anisotropy of the form $\tilde{J}_3 = K_3 l^2 / \rho^2$ leads to exact solutions for $\Theta(\rho)$. Here, K_3 is the strength of the anisotropy and l is the length scale characterizing the inhomogeneity. Using this form of \tilde{J}_3 , we find the Euler-Lagrange variational equation corresponding to Eq. (4). Changing variables to $\tilde{\rho} = \ln(\rho/\rho_0)$ [22] in this equation where ρ_0 is a constant, we get

$$\partial^2 \Theta / \partial \tilde{\rho}^2 = \frac{1}{2} (\alpha_0^2 + K_3 l^2 \beta_0^2) \sin 2\Theta. \quad (5)$$

Imposing the periodic boundary conditions $\Phi(\phi + 2\pi) = \Phi(\phi)$ and $\Phi(z + L) = \Phi(z)$, we find $\alpha_0 = n$, $\beta_0 = 2\pi m/L$ where m and n are integers. Equation (5) then yields, for the function $\tilde{\Theta} = 2\Theta$,

$$\partial^2 \tilde{\Theta} / \partial \tilde{\rho}^2 = \mu^2 \sin \tilde{\Theta} \quad (6)$$

with the solution $\tilde{\Theta}(\tilde{\rho}) = 4 \tan^{-1}(e^{\mu \tilde{\rho}})$, where

$$\mu = \pm (n^2 + 4K_3 \pi^2 m^2 l^2 / L^2)^{1/2}. \quad (7)$$

In terms of the original variables, the solution for Θ reads

$$\Theta(\rho) = 2 \tan^{-1}[(\rho/\rho_0)^\mu]. \quad (8)$$

Using Eq. (2), we arrive at the exact static solution in 3D for the spin configuration,

$$\mathbf{S}(\rho, \phi, z) = \left(\frac{2(\rho/\rho_0)^\mu}{1 + (\rho/\rho_0)^{2\mu}} \cos \Phi(\phi, z), \frac{2(\rho/\rho_0)^\mu}{1 + (\rho/\rho_0)^{2\mu}} \sin \Phi(\phi, z), \frac{1 - (\rho/\rho_0)^{2\mu}}{1 + (\rho/\rho_0)^{2\mu}} \right), \quad (9)$$

where $\Phi(\phi, z) = n\phi + 2\pi mz/L + \Phi_0$, with $\Phi_0 = \Phi(0, 0)$. We note that the solution for $\mathbf{S}(\mathbf{r})$ depends on the two integers n and m .

If $\mu < 0$, then as $\rho \rightarrow 0$, we find $\Theta(\rho) \rightarrow \pi$ and $\mathbf{S} \rightarrow (0, 0, -1)$; while as $\rho \rightarrow \infty$, we have $\Theta(\rho) \rightarrow 0$ and hence $\mathbf{S} \rightarrow (0, 0, 1)$. When $\rho = \rho_0$, $\Theta = \pi/2$. In the plane $z = 0$, the solution becomes a *modified* skyrmion (resp., antiskyrmion) for $n > 0$ (resp., $n < 0$). (The modification arises from the presence of the anisotropy K_3 in the exponent μ .) Its winding number (topological charge) Q can be computed, to obtain $-n$ and $+n$, respectively [23]. An inspection of Eq. (9) shows that the skyrmion twists out into the z direction in a periodic fashion.

The occurrence of μ as the exponent of (ρ/ρ_0) in the soliton solution (9) is of significance. The form and geometry of the topological solution we have obtained depend strongly on the material parameters K_3 and l/L that appear in μ , representing respectively the effects of anisotropy and inhomogeneity in the interacting system of spins. The presence of μ enables us to control the rate of change of $\Theta(\rho)$ with ρ in the soliton solution, by tuning these material parameters. This in turn should be helpful in designing experiments to create and observe the 3D soliton.

For completeness, we point out that if $\mu > 0$ in Eq. (9), the spin configuration for $z = 0$ corresponds to $\mathbf{S} \rightarrow (0, 0, 1)$ as $\rho \rightarrow 0$, while $\mathbf{S} \rightarrow (0, 0, -1)$ as $\rho \rightarrow \infty$. Some authors [13] use this alternative boundary condition to define a skyrmion. All the results in the foregoing hold good for both conventions. We also note that the homogeneous boundary condition on $\mathbf{S}(\mathbf{r})$ in each $z = \text{constant}$ plane, together with the periodicity in the z -direction, imply [24] that our soliton represents a map $\mathbf{S} : S^2 \times T^1 \rightarrow S^2$.

Calculation of the Hopf invariant. Next, we show that the Hopf invariant H for this exact 3D static soliton is an integer. Hence the solution given by Eq. (9) is a hopfion. As mentioned in the Introduction,

H can be calculated from the Whitehead formula [14, 25]

$$H = -(1/8\pi^2) \iiint (\mathbf{A} \cdot \mathbf{B}) dx dy dz, \quad (10)$$

where the Cartesian components of the ‘emergent magnetic field’ [1] are given by $B_x = -\mathbf{S} \cdot (\partial_y \mathbf{S} \times \partial_z \mathbf{S})$ and cyclic permutations for B_y and B_z , and \mathbf{A} is the corresponding vector potential. It is easily verified that $\nabla \cdot \mathbf{B} = 0$. Using the solution (9) and expressing the Cartesian components of \mathbf{B} in cylindrical polar coordinates in physical space, we get

$$B_x = \beta_0(\partial_\rho \cos \Theta) \sin \phi, \quad B_y = -\beta_0(\partial_\rho \cos \Theta) \cos \phi, \quad B_z = (\alpha_0/\rho)\partial_\rho \cos \Theta. \quad (11)$$

Solving $\nabla \times \mathbf{A} = \mathbf{B}$ for the Cartesian components of \mathbf{A} using the appropriate boundary conditions on $\Theta(\rho)$ [as described below Eq. (9)], a lengthy but straightforward calculation yields

$$A_x = -(\alpha_0/\rho)(\cos \Theta \pm 1) \sin \phi, \quad A_y = (\alpha_0/\rho)(\cos \Theta \pm 1) \cos \phi, \quad A_z = \beta_0 \cos \Theta. \quad (12)$$

The \pm signs correspond to $\mu > 0$ and $\mu < 0$, respectively. Substituting Eq. (11) and Eq. (12) in Eq. (10), the Hopf invariant of the 3D soliton can be written in the form

$$H = \mp \frac{\alpha_0 \beta_0}{8\pi^2} \int_0^L dz \int_0^{2\pi} d\phi \int_0^\pi \sin \Theta d\Theta. \quad (13)$$

Since $\alpha_0 = n$ and $\beta_0 = 2\pi m/L$, we obtain

$$H = nm, \quad (14)$$

keeping in mind that n can be a positive or negative integer. Since H is an integer, the soliton is a hopfion. Interestingly, this integer emerges as a product of two integers in our spin system. As H can have either sign, the system supports both hopfions and anti-hopfions.

Knotted structure of the hopfion and Hopf invariant as a linking number. Next, we use *Mathematica* to find the preimage of any specific point on S^2 , i.e., the points in 3D space corresponding to a specific value (Θ, Φ) of $\mathbf{S}(\mathbf{r})$ of the hopfion solution (9). We have plotted the three preimage curves corresponding to $\Theta = \pi/2$ and $\Phi = 0, \pi/3$ and $2\pi/3$, for the cases (i) $n = 1, m = 1$ [Fig. 1(a)], (ii) $n = 1, m = 2$ [Fig. 1(b)], and (iii) $n = 3, m = 2$ [Fig. 1(c)]. As these illustrative examples show, each of the preimages is a closed space curve which is, in cases (i) and (ii), an unknot, topologically equivalent to a circle. In contrast, it

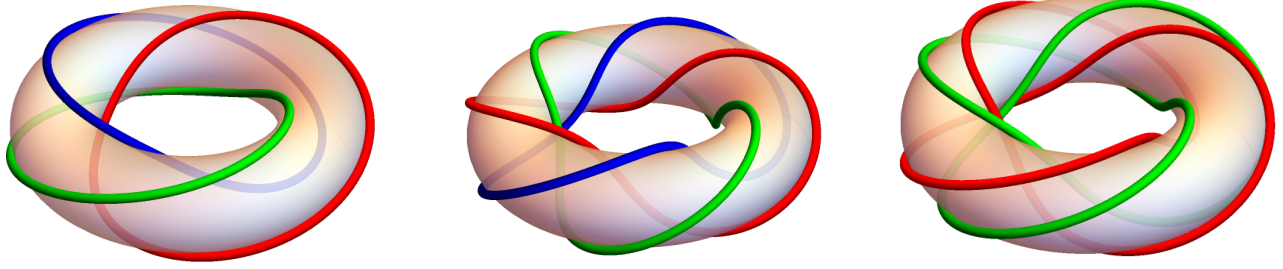


Figure 1: Preimages on a torus for a hopfion [Eq. (9)]. (a) Left panel: $n = 1, m = 1$, unknots, linking number $H = 1$. (b) Middle panel: $n = 1, m = 2$, unknots, linking number $H = 2$. (c) Right panel: $n = 2, m = 3$, trefoil knots, linking number $H = 6$.

is a trefoil knot (a nontrivial knot) in case (iii). Further, as can be readily seen in Fig. 1, each closed curve lies on the surface of a torus, traversing n times around the poloidal direction and m times around the toroidal direction. The analytical result of Eq. (14) gives $H = 1, 2, 6$, respectively in cases (i), (ii) and (iii). Correspondingly, we see from Fig. 1 that any two closed space curves link once, twice and six times, respectively, in these three cases. This corroborates geometrically that the Hopf invariant H is precisely just the *linking number* of the preimages of two distinct points on S^2 . For a given value of Θ , the preimages of the points $\Phi \in [0, 2\pi)$ densely fill the corresponding torus (Fig. 2). As is well known [26], a torus knot is an unknot if and only if either n or m is ± 1 , and a nontrivial knot if m and n are coprime. Our plots illustrate the knotted and linked structure of the hopfion.

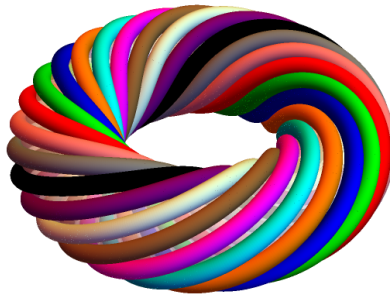


Figure 2: A torus densely filled by the preimages of the points on a fixed latitude of S^2 . Different colors correspond to different points on the latitude.

Exact hopfion energy and its topological lower bound. Next, we calculate the energy of a hopfion exactly. Setting $\tilde{J}_3 = K_3 l^2 / \rho^2$ in Eq. (4), using the definition of μ from Eq. (7) and putting in the appropriate limits of integration, the energy of the hopfion is given by

$$E = (J/a) \int_0^L dz \int_0^{2\pi} d\phi \int_0^\infty \{ \rho (\partial_\rho \Theta)^2 + \mu^2 \rho^{-1} \sin^2 \Theta \} d\rho. \quad (15)$$

Using Eq. (8) for $\Theta(\rho)$, a short calculation yields

$$E = \frac{16\pi JL}{a} \mu^2 \rho_0^{2\mu} \int_0^\infty \frac{\rho^{(2\mu-1)}}{[\rho_0^{2\mu} + \rho^{2\mu}]^2} d\rho = (8\pi JL/a) |\mu|. \quad (16)$$

Substituting for μ from Eq. (7), the hopfion energy is given by the exact expression

$$E(n, m) = (8\pi JL/a) (n^2 + 4\pi^2 K_3 l^2 m^2 / L^2)^{1/2}. \quad (17)$$

Since $E(n, m) = E(-n, m)$, hopfions and anti-hopfions have the same energy. It follows on simple grounds from Eq. (17) that the topological lower bound on E is given by

$$E \geq c |H|^{1/2}, \quad (18)$$

where $c = 2^{17/4} \pi^2 K_3^{-1/2} J l / a$. Thus, the lower bound on the hopfion energy has a *sublinear* dependence on its topological charge H . This is in contrast to the well known lower energy bound for the skyrmion, which is linear in the Pontryagin charge Q . Such a sublinear behavior is usually attributed [27] to the knotted and linked preimages, which is the source of the charge H of the hopfion.

Discussion. The main results obtained in this Letter have already been summarized in the Introduction. Our results are novel and we believe they open up new avenues of investigation, e.g. hopfion lattice solutions of the model, study of the effects of an applied magnetic field on hopfions, topological transitions in spin textures, Berry phase phenomena and the dynamics of hopfions.

In order to investigate the stability of our 3D hopfion given in Eq. (9), we carry out the usual Hobart-Derrick analysis [28], after substituting $\tilde{J}_3 = K_3 l^2 / \rho^2$ in Eq. (1) for the energy E . On letting $(x, y, z) \rightarrow (\lambda x, \lambda y, \lambda z)$, the first two terms scale linearly in λ , while the third scales as λ^{-1} . This leads to a minimum in the energy at a nonzero value of λ , implying stability of the topological soliton.

It has been shown in the case of chiral ferromagnets [19] and chiral ferromagnetic fluids [29] that the presence of the Dzyaloshinskii-Moriya interaction term [30] $D \mathbf{S} \cdot (\nabla \times \mathbf{S})$ in the energy plays an important

role in stabilizing the hopfion. Turning to nonchiral (inversion symmetric) ferromagnets, it is reasonable to expect that continuum Heisenberg models with competing energy terms could lead to stable solitons. However, identifying appropriate terms which would yield a soliton solution with integer Hopf invariant is far from obvious. Further, unlike chiral magnets, such inversion symmetric magnets support both hopfions and anti-hopfions, thereby leading to richer topological aspects that can be useful in technological applications.

The introduction of an inhomogeneity in the exchange interaction in a Heisenberg model was motivated in part by earlier work [31] on the dynamics of the continuum model of an isotropic Heisenberg chain with an inhomogeneous exchange interaction. Since then, various aspects of inhomogeneous magnetic systems have been studied [32]. We remark in passing that the results we have presented for the continuum Heisenberg model should be applicable in fields other than magnetism, where the corresponding Hamiltonian density involves inhomogeneous, anisotropic generalizations of $|\nabla\mathbf{n}|^2$, where \mathbf{n} is a unit vector field. The energy density of the nonlinear sigma model [7], the splay term in the free energy of liquid crystals [4], the curvature term in the elastic rod energy [33], etc. are some examples.

Theoretical and experimental studies of magnetic hopfions in 3D Heisenberg models have started to gain momentum in recent years. Hopfions have been identified using fluorescence polarizing microscopy in a chiral ferromagnetic fluid by the twisting and linking of the magnetization field lines [29]. Recently, they have been created and observed [1] in magnetic multilayer systems. Based on their nanometer to micrometer sizes in various magnetic materials and their topological stability, the possible application of hopfions in future computer technology has been recognized. They can be used to store bits of information, where a bit corresponds to the presence or absence of a hopfion, or the presence of a hopfion and an anti-hopfion in nonchiral magnets. Certain dynamical advantages of hopfions over skyrmions as information carriers have also been pointed out [21]. Thus, one could envisage such distinct applications as *hopfionics* akin to the field of skyrmionics [13].

We conclude by pointing out that our magnetic model is not just an exactly solvable theoretical model that reveals all the topological aspects of hopfions succinctly, but is also useful in designing novel experiments to observe them. Specifically, we note that the J_3 term in the energy Eq. (1) has the same effect as

a perpendicular magnetic anisotropy (PMA) term KS_z^2 used in experiments. Hopfions with hopf charge $H = 1$ have been studied in Ir/Co/Pt nano-disc multilayered systems, with the PMA term K varying spatially over each layer, with a linear dependence [1]. Our results suggest that layers with a circularly symmetric inverse square dependence $1/\rho^2$ of the inhomogeneity in the anisotropy, will lead to stable hopfions with a range of H values. Finally, we note that the inverse square interaction of our model that has led to exact solvability is *reminiscent* of the similar interaction (in a different context) between particles in the well known Calogero-Moser model which is known to be completely integrable, with connections to diverse fields [34]. Hence our work has potential ramifications for other physical systems as well. We hope that our results will motivate the fabrication of inhomogeneous, anisotropic 3D magnetic materials that are described by our model, so that the exact hopfions predicted by it can be created in the laboratory and their possible applications in nanotechnology investigated.

Acknowledgments.— We thank Ayhan Duzgun for help with the figures. The work of A.S. at Los Alamos National Laboratory was carried out under the auspices of the U.S. DOE and NNSA under Contract No. DEAC52-06NA25396.

References

- [1] N. Kent *et al.*, Nature Commun. **12**, 1562 (2021).
- [2] I. Luk’yanchuk, Y. Tikhonov, A. Razumna, and V. M. Vinokur, Nature Commun. **11**, 2433 (2020).
- [3] P. J. Ackerman and I. I. Smalyukh, Nature Commun. **12**, 1562 (2021). Nature Mater. **16**, 426 (2017).
- [4] P. J. Ackerman and I. I. Smalyukh, Phys. Rev. X **7**, 011006 (2017).
- [5] Y. M. Bidasyuk *et al.*, Phys. Rev. A **92**, 053603 (2015).
- [6] S. Zou *et al.*, Phys. Fluids **33**, 027105 (2021).
- [7] R. Rajaraman, *Solitons and Instantons* (North-Holland, Amsterdam, 1982).
- [8] N. Manton and P. Sutcliffe, *Topological Solitons* (Camb. Univ. Press, Cambridge, 2004), and references therein.

- [9] T. Dauxois and M. Peyard, *Physics of Solitons* (Camb. Univ. Press, Cambridge, 2006).
- [10] Y. M. Shnir, *Topological and Nontopological Solitons in Scalar Field Theories* (Camb. Univ. Press, Cambridge, 2018).
- [11] A. M. Kosevich, B. A. Ivanov, and A. S. Kovalev, Phys. Rep. **194**, 117 (1990).
- [12] A. A. Belavin and A. M. Polyakov, JETP Lett. **22**, 245 (1975).
- [13] For reviews of magnetic skyrmions see, e.g., N. Nagaosa and Y. Tokura, Nat. Nanotechnol. **8** 899 (2013); A. Fert, N. Reyren, and V. Cros, Nat. Rev. Mater. **2** 17031 (2017); B. Göbel, I. Mertig, and O. A. Tretiakov, Phys. Rep. **895**, 1 (2021), and references therein.
- [14] J. H. C. Whitehead, Proc. Nat. Acad. Sci. (USA) **33**, 117 (1947).
- [15] P. Sutcliffe, Phys. Rev. Lett. **118** 247203 (2017).
- [16] P. Sutcliffe, Nat. Mater. **16**, 392 (2017).
- [17] P. Sutcliffe, Rev. Math. Phys. **30**, 1840017 (2018).
- [18] M. Kobayashi and M. Nitta, Phys. Lett. B **728**, 314 (2014).
- [19] Y. Liu, R. K. Lake, and J. Zang, Phys. Rev. B **98**, 174437 (2018).
- [20] F. N. Rybakov, N. S. Kiselev, A. B. Borisov, L. Döring, C. Melcher, and S. Blügel, arXiv:1904.00250.
- [21] X. S. Wang, A. Quaimzadeh, and A. Brataas, Phys. Rev. Lett. **123**, 147203 (2019).
- [22] A. Saxena and R. Dandoloff, Phys. Rev. B **66**, 104414 (2002).
- [23] See, e.g., W. Koshibae and N. Nagaosa, Nat. Commun. **7**, 10542 (2016).
- [24] J. Jaykka and J. Hietarinta, Phys. Rev. D **79**, 125027 (2009) and references therein.
- [25] J. Gladikowski and M. Helmund, Phys. Rev. D **56**, 5194 (1997).
- [26] See, e.g., C. Oberti and L. Ricca, J. Knot Theory Ramif. **25**, 1650036 (2016).

- [27] R. S. Ward, J. Math. Phys. **59**, 022904 (2018).
- [28] R. H. Hobart, Proc. Phys. Soc. **82**, 201 (1963); G. M. Derrick, J. Math. Phys. **5**, 1252 (1964).
- [29] P. J. Ackerman and I. I. Smalyukh, Nat. Mater. **16**, 426 (2017).
- [30] I. Dzyaloshinskii, J. Phys. Chem. Solids **4**, 241 (1958); T. Moriya, Phys. Rev. **120**, 91 (1960).
- [31] Radha Balakrishnan, J. Phys C: Solid State Phys. **15**, L 1305 (1982).
- [32] See, e.g., Z-H. Zhang *et al.* J. Phys. Soc. Jpn. **75**, 104002 (2006); K. H. Han and H. J. Shin, J. Phys. A: Math. Theor. **40**, 979 (2007); K. Abhinav and P. Guha, Eur. Phys. J. B, 91:52 (2018); M. Saravanan and W. B. Cardoso, Commun. Nonlinear Sci. Numer. Simulat. **69**, 176 (2019); Y-J. Zhang, D. Zhao, and Z-D. Li, Commun. Theor. Phys. **73**, 015105 (2021).
- [33] D. Harland, M. Speight, and P. Sutcliffe, Phys. Rev. D **83**, 065008 (2011).
- [34] F. Calogero, J. Math. Phys. **12**, 419 (1971) [*Erratum*, *ibid*; 3646 (1996)]; J. Moser, Advances in Math. **16**, 197 (1975); See also, P. Etingof, Lectures on Calogero-Moser Systems, arXiv:math/0606233.